

Intrinsic phonon relaxation times from first-principles studies of the thermal conductivities of Si and Ge

A. Ward and D. A. Broido

Department of Physics, Boston College, Chestnut Hill, Massachusetts 02467, USA

(Received 23 December 2009; published 4 February 2010)

Using a first-principles approach, we present forms for the intrinsic phonon relaxation times in semiconductors, which properly reflect the physically distinct behaviors of the normal and umklapp scattering processes. We find that accurate representation of the phonon-phonon scattering strength and inclusion of scattering of acoustic phonons by optic phonons are essential ingredients, which are missing from the decades old derivations of commonly used intrinsic relaxation times. We also assess the validity of the relaxation time approximation itself for silicon and germanium.

DOI: [10.1103/PhysRevB.81.085205](https://doi.org/10.1103/PhysRevB.81.085205)

PACS number(s): 71.15.Mb, 63.20.kg, 66.70.-f

I. INTRODUCTION

Phonon-phonon scattering is an intrinsic scattering mechanism that dominates the behavior of the lattice thermal conductivity, κ_L , for crystalline semiconductors and insulators around and above room temperature. For over half a century, models of phonon thermal transport in bulk and nanostructured materials¹⁻¹¹ have commonly employed relaxation times for phonon-phonon scattering to bypass the difficulty in solving the phonon Boltzmann transport equation (BTE) first introduced by Peierls many years ago.¹² The lowest order phonon-phonon scattering process occurs between three phonons. The pioneering work of Klemens,¹ Herring,² Callaway,³ Holland,⁴ and Slack⁵ presented relaxation times due to three-phonon scattering, which were taken to have the form: $\tau^{-1}(\omega, T) = A\omega^n f(T)$, where ω is the phonon frequency, n is an integer, $f(T)$ is one of several temperature-dependent functions, and A is a constant usually determined by fitting to experimental thermal conductivity data. These relaxation times were originally derived using models that implicitly assumed small phonon frequencies and low temperature where the resistive umklapp scattering processes are weak. Specifically, (a) only acoustic phonon branches were included within a Debye approximation; optic phonon branches were omitted and (b) the three-phonon scattering strength was modeled taking all three acoustic phonons to have low frequency, an assumption that is incompatible with the very umklapp scattering processes that produce the thermal resistance. During the subsequent decades, these relaxation times have attained widespread usage to describe high temperature thermal transport in materials, outside the temperature domain for which they were constructed. Furthermore, since phonon-phonon scattering is an inelastic process, the validity of the relaxation-time approximation (RTA) itself needs to be assessed in order to validate its ubiquitous use.

Recently, we have developed an *ab initio* approach to calculate κ_L around and above room temperature.^{13,14} This approach combines first-principles calculations of harmonic and anharmonic interatomic force constants (IFCs) using density-functional perturbation theory¹³⁻¹⁶ (DFPT) with an exact numerical solution of the BTE.^{13,14,17,18} Thus, the full phonon dispersions *and* the quantum mechanical three-phonon scattering rates are accurately represented throughout

the Brillouin zone *without introducing any adjustable parameters*. This differentiates our approach from recent first-principles molecular dynamics simulations,⁸ which approximate the phonon-phonon scattering using an *ad hoc* relaxation time. We have applied our *ab initio* theory to silicon, germanium and diamond, and we have achieved excellent agreement with measured κ_L data for these materials.^{13,14}

In this paper, we use our accurate, parameter-free approach to construct intrinsic phonon relaxation times by explicitly fitting to data obtained from our *ab initio* calculations for Si and Ge. We determine relaxation times for both transverse acoustic (TA) and longitudinal acoustic (LA) branches, and in each case, for both momentum conserving normal (N) and momentum nonconserving umklapp (U) scattering. We find functional forms for the relaxation times, which reveal the physically motivated distinct behaviors of the N and U processes.

In Sec. II we present our first-principles-based approach to formulate the intrinsic phonon relaxation times. Section III gives the results obtained and discusses them. A summary and conclusions is presented in Sec. IV.

II. THEORY

The relaxation time for phonon mode λ , τ_λ^{RTA} , can be expressed as $\tau_\lambda^{RTA} = n_\lambda^0(n_\lambda^0 + 1)/Q_\lambda$, where n_λ^0 is the Bose distribution function and Q_λ is the diagonal part of the three-phonon collision operator:^{13,14,17-19}

$$Q_\lambda = \sum_{\lambda' \lambda''} \left(W_{\lambda\lambda'\lambda''}^+ + \frac{1}{2} W_{\lambda\lambda'\lambda''}^- \right). \quad (1)$$

Here λ is a short hand for (j, \vec{q}) , the branch index and phonon wave vector, respectively, and $W_{\lambda\lambda'\lambda''}^\pm$ are the scattering rates for three-phonon processes. The sum in Eq. (1) is over the phase space of λ' and λ'' that satisfy momentum and energy conservation: $\vec{q} \pm \vec{q}' = \vec{q}'' + \vec{K}$, where \vec{K} is a reciprocal lattice vector, and $\omega_j(\vec{q}) \pm \omega_{j'}(\vec{q}') = \omega_{j''}(\vec{q}'')$. We calculate this phase space explicitly including all phonon branches for a fine grid of \vec{q} values throughout the Brillouin zone following the method described in Refs. 13, 14, 17, and 18. Relaxation

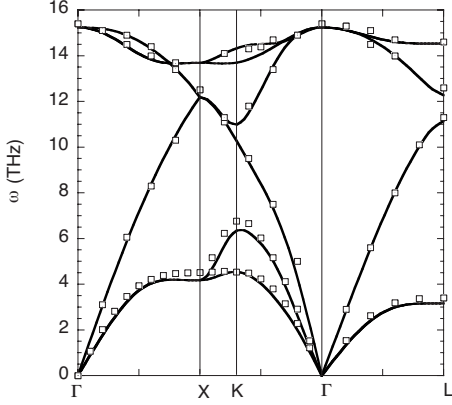


FIG. 1. Calculated phonon dispersion of silicon along high-symmetry directions compared to measured data from Ref. 22.

times for both N and U processes are obtained by decomposing Q_λ as $Q_\lambda = Q_\lambda^{(N)} + Q_\lambda^{(U)}$ where the terms in the sum in Eq. (1) have been separated according to whether they correspond to N or U scattering events. The corresponding relaxation times are then given by $\tau_\lambda^{(i)} = n_\lambda^0(n_\lambda^0 + 1)/Q_\lambda^{(i)}$, for $i=N$ and $i=U$, and the total relaxation time, τ_λ^{RTA} , reflects Matthiessen's rule: $1/\tau_\lambda^{RTA} = 1/\tau_\lambda^{(N)} + 1/\tau_\lambda^{(U)}$.

Determination of τ_λ^{RTA} allows calculation of the RTA lattice thermal conductivity, $\kappa_L^{RTA}(T)$, as a sum of per branch contributions:²⁰ $\kappa_L^{RTA}(T) = \sum_j \kappa_j^{RTA}(T)$, with

$$\kappa_j^{RTA}(T) = \frac{1}{3} \frac{1}{(2\pi)^3} \int C[\omega_j(\vec{q})] v_j^2(\vec{q}) \tau_j^{RTA}(\vec{q}) d\vec{q}, \quad (2)$$

where the mode specific heat is $C(\omega_\lambda) = k_B(\hbar\omega_\lambda\beta)^2 n_\lambda^0(n_\lambda^0 + 1)$, and v_λ is the phonon velocity in mode λ .

The $W_{\lambda\lambda'\lambda''}^\pm$ depend on the phonon frequencies, eigenvectors, and the strength of the lattice anharmonicity. The only inputs needed to calculate these quantities and hence τ_λ^{RTA} are the harmonic and anharmonic IFCs. We obtain these IFCs from first-principles using DFPT.¹³⁻¹⁶ The Quantum Espresso package²¹ is used to calculate ground-state energies and harmonic IFCs, while the anharmonic IFCs have been generated for triplet interactions out to seventh nearest neighbors, exploiting the $2n+1$ theorem¹⁵ and following the method described in Ref. 16. Figure 1 shows the calculated phonon dispersion for Si along high symmetry directions compared to experiment highlights the accuracy of the first-principles approach.

Using this *ab initio* based approach, we have calculated $\tau_j^{(N)}(\vec{q})$ and $\tau_j^{(U)}(\vec{q})$ for Si and Ge for the three acoustic phonon branches. This process is repeated for a wide range of temperatures, $\Theta_D/4$ to $2\Theta_D$, where Θ_D is the Debye temperature. Since the pair, (j, \vec{q}) , define a frequency, ω , these relaxation times are transformed to frequency and temperature-dependent functions $\tau_j^{(N)}(\omega, T)$ and $\tau_j^{(U)}(\omega, T)$.²³ For high temperatures, the Bose factors in the scattering rates, $W_{\lambda\lambda'\lambda''}^\pm$, all take the form, $n_\lambda^0 \sim k_B T / \hbar\omega_\lambda$, which gives an explicit separation in the frequency and temperature dependence: $\tau_j^{(i)}(\omega, T) \sim 1/f^{(i)}(\omega)T$, where $f^{(i)}(\omega)$ contains only

TABLE I. Silicon and germanium for N and U relaxation time coefficients for LA and TA branches.

	$A_{TA}^{(N)}$ (meV ² K s) ⁻¹	$A_{LA}^{(N)}$ (meV ² K s) ⁻¹	$A_{TA}^{(U)}$ (meV ⁴ K s) ⁻¹	$A_{LA}^{(U)}$ (meV ⁴ K s) ⁻¹
Si	253322	163921	2012	507
Ge	460248	401980	8634	1990

frequency dependence. The high-temperature limit $\tau_\lambda^{(i)} \sim T^{-1}$ means, from Eq. (1), that $\kappa_L \sim T^{-1}$, which is characteristic of the three-phonon scattering limited κ_L . We therefore model the N and U relaxation times with the commonly used product form: $\tau_j^{(i)}(\omega, T) \sim 1/[A_j^{(i)} \omega^{n_i} g^{(i)}(T)]$, which is a natural choice for the temperature regime considered here. It is clear, however, that for the original low-temperature RTA models,¹⁻⁵ this form is only valid for frequencies sufficiently low that $k_B T / \hbar\omega_\lambda \gg 1$.

Using the high-temperature *ab initio* values of $\tau_j^{(i)}(\omega, T)$, we are able to fit the frequency dependence for both Si and Ge using integers for the exponents: $n_N \approx 2$ and $n_U \approx 4$. Then the functions, $g^{(i)}(T)$, are fit to the *ab initio* relaxation times and thermal conductivity data over the full temperature range considered. For all acoustic branches and for both N and U processes, the data is well described by the single function, $g(T) = T[1 - \exp(-3T/\Theta_D)]$. Finally, since the relaxation times and per branch contributions to $\kappa_j^{RTA}(T)$ for each TA branch are close, the coefficients $A_j^{(i)}$ for $j=TA_1$ and $j=TA_2$ are assumed to be identical. The remaining four coefficients, $A_{TA}^{(N)}$, $A_{TA}^{(U)}$, $A_{LA}^{(N)}$, and $A_{LA}^{(U)}$, are adjusted to best fit the *ab initio* relaxation time and thermal conductivity data. The final forms are: $\tau_j^{(N)}(\omega, T) = 1/\{A_j^{(N)} \omega^2 T [1 - \exp(-3T/\Theta_D)]\}$ and $\tau_j^{(U)}(\omega, T) = 1/\{A_j^{(U)} \omega^4 T [1 - \exp(-3T/\Theta_D)]\}$. The values for the coefficients for Si and Ge are given in Table I.

III. RESULTS AND DISCUSSION

Figure 2 shows the thermal conductivity contributions, $\kappa_{TA_1}^{RTA}(T) + \kappa_{TA_2}^{RTA}(T)$, for the combined TA branches, and

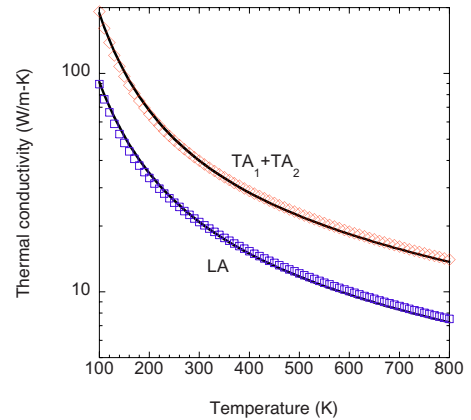


FIG. 2. (Color online) Temperature dependence of the TA and LA contributions to the intrinsic lattice thermal conductivity of Ge: blue open squares: LA branch *ab initio* results; red diamonds: combined TA *ab initio* results; solid black curves: RTA results.

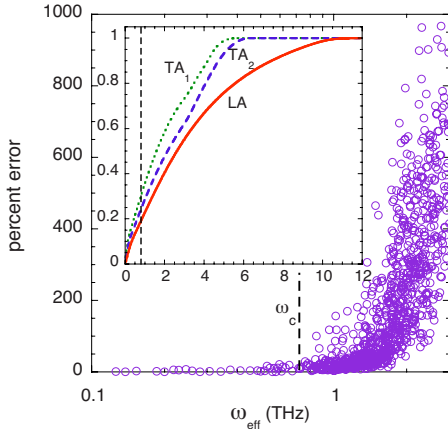


FIG. 3. (Color online) Percent error in $|\Phi_{\lambda\lambda'\lambda''}|^2$ using the LWA compared to *ab initio*, as described in text. Inset shows percent contributions to TA and LA phonon branch thermal conductivities for Si vs phonon frequency at $T=300$ K.

$\kappa_{LA}^{RTA}(T)$ for the LA branch, for Ge. The solid curves show results obtained using the approximate RTA functional form described above, while the open squares and diamonds give the corresponding results obtained from the full *ab initio* calculations. The agreement is very good over the full temperature range reflecting the accurate representation of the N and U phonon-phonon scattering. Similarly good results are obtained for Si.

In principle, phonon frequencies depend on temperature because thermal expansion causes the lattice constant to increase. However, our ground state and IFC calculations were performed at zero temperature. We have investigated the effect of lattice constant changes by calculating τ_{λ}^{RTA} using IFCs determined from a range of lattice constants consistent with the temperature range considered here. We find for both Si and Ge that τ_{λ}^{RTA} is relatively insensitive to such changes, producing only small shifts in the thermal conductivity ($\sim 1\% - 2\%$).

Our first-principles approach allows us to examine some of the assumptions made in the early RTA theories. Since we explicitly calculate millions of three-phonon processes for all phonon branches and throughout the Brillouin zone, we are able to assess the importance of (a) use of the low-frequency approximation for three-phonon scattering, (b) including the optic phonons, and (c) use of the full dispersive and anisotropic phonon branches.

The strength of each three-phonon scattering process is governed by the corresponding matrix element, $\Phi_{\lambda\lambda'\lambda''}$.^{13,14,16-19} Commonly used intrinsic relaxation times have been derived using the long wavelength approximation (LWA) for acoustic phonons: $\Phi_{\lambda\lambda'\lambda''} \sim qq'q''$ with $q, q', q'' \ll 1/a$, where a is the lattice spacing. However, we find that the LWA holds for only a small fraction of the phase space of three-phonon scattering events. This is illustrated in Fig. 3, which shows the percent error between the $|\Phi_{\lambda\lambda'\lambda''}|^2$ from our *ab initio* calculations and that using the LWA for a representative selection of momentum and energy conserving $TA_1 + TA_2 \rightarrow LA$ processes in Si throughout the Brillouin zone, and taking $T=300$ K. We have plotted this error as a function of $\omega_{eff} = [\omega_{TA1}(\vec{q})\omega_{TA2}(\vec{q}')\omega_{LA}(\vec{q}'')]^{1/3}$, which gives a

measure of how far the phonons participating in a scattering event are from the zone center. It is clear from the figure that the LWA works poorly for $\omega_{eff} > \omega_c$ where ω_c is indicated by the short vertical dashed line. The inset shows the percent contributions to κ_{TA1}^{RTA} , κ_{TA2}^{RTA} , and κ_{LA}^{RTA} as a function of ω . The dashed line is at $\omega = \omega_c$. The failure of the LWA is highlighted by the fact that the majority of the contributions to κ_{TA1}^{RTA} , κ_{TA2}^{RTA} , and κ_{LA}^{RTA} come for $\omega > \omega_c$ (right of dashed line) where the LWA $\Phi_{\lambda\lambda'\lambda''}$ is no longer valid.

Optic modes are typically ignored in RTA models because they carry far less heat than phonons deriving from the acoustic branches. This point is borne out by our first-principles calculations^{13,14} where we find for both Si and Ge that less than 10% of the heat is carried by the optic branches at room temperature. However, the optic modes play an essential role in providing scattering channels for the heat-carrying acoustic phonons. In fact, between 50% and 60% of the total scattering processes involving acoustic phonons in Si and Ge include at least one optic phonon. Removal of the acoustic-optic phonon (*a-o*) scattering channels in our first-principles calculations increases κ_L dramatically. For example, such removal increases the calculated κ_L of Si by more than a factor of three from (145W/mK to 501W/mK) at 300K. It is therefore conceptually and quantitatively incorrect to exclude *a-o* scattering in developing an intrinsic phonon relaxation time model appropriate for room and higher temperatures. We find that doing so changes not only the coefficients, $A_j^{(i)}$, in Table I but also the frequency and temperature dependence of τ_{λ}^{RTA} .

The TA and LA relaxation times have been extracted using the *ab initio* phonon dispersions throughout the Brillouin zone. This was essential in determining the correct frequency dependences and coefficients, as highlighted above in the context of *a-o* scattering. We note, however, that for calculating the contributions, κ_j^{RTA} in Eq. (2), these relaxation times can be used with a Debye model for the phonon dispersions instead of the *ab initio* dispersions. For both Si and Ge, we find less than a 10% difference in doing so over the full temperature range shown in Fig. 2.

Our first-principles approach to phonon thermal transport uses an exact numerical solution of the BTE,^{13,14} allowing us to assess the significance of using the RTA approach developed here. For Si and Ge, we find that κ_L is only $\sim 5\% - 10\%$ larger than κ_L^{RTA} over the temperature range considered. Thus, for these materials the RTA approach described above works quite well. In contrast, at low temperatures and for materials where umklapp scattering is weak, the difference between κ_L and κ_L^{RTA} can be quite large. For example, in isotopically enriched diamond, κ_L is about 50% larger than κ_L^{RTA} at $T=300$ K (see Fig. 2 in Ref. 14). We note that κ_L must always be larger than κ_L^{RTA} because, as constructed, the RTA treats $\tau^{(N)}$ as an independent resistive process, but it is well known that N scattering alone does not provide thermal resistance. The Callaway model^{3,20} constructs a correction term $\Delta\kappa_C$ within an RTA. Inserting our calculated intrinsic relaxation times for Si and Ge into the Callaway model, we find $\Delta\kappa_C$ to be small ($< 6\%$ for 300K) consistent with our *ab initio* results.

Previous unavailability of first-principles results has led to erroneous conclusions being reached from RTA models. For

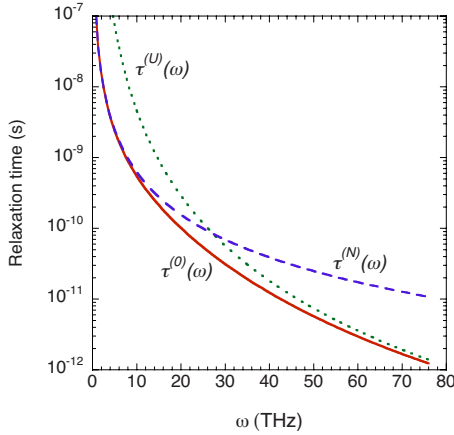


FIG. 4. (Color online) Normal (blue dashed curve), umklapp (green dotted curve), and total (red solid curve) relaxation times as a function of angular frequency for the LA branch of Si at $T=300$ K.

example, it has been argued that N scattering dominates in defect-free Ge even at relatively high temperatures⁶ and that $\Delta\kappa_C(T)$ is therefore correspondingly large. This is contrary to our findings above and contrary to what one would expect for most materials. Physical reasoning dictates that N scattering processes should dominate the behavior of the relaxation time in the low-frequency range where few long wavelength phonons can find partners that satisfy momentum and energy conservation conditions for U scattering. But, with increasing frequency, one would expect U scattering to become increasingly important as shorter wavelength phonons can readily find U scattering partners. Thus, in the temperature range where phonon-phonon scattering dominates the behavior of κ_L , a frequency cross-over region should exist for *any* RTA model of this intrinsic scattering mechanism where the total relaxation time is governed by N scattering for low frequency and U scattering at high frequency.

Our *ab initio* results reveal this behavior. This is illustrated in Fig. 4 for the LA branch in Si for $T=300$ K. The dashed blue curve shows $\tau_{LA}^{(N)}(\omega)$ and the dotted green curve shows $\tau_{LA}^{(U)}(\omega)$. The total relaxation time, $\tau_{LA}^{RTA}(\omega)$, is given by the solid red curve. The stronger frequency dependence of $\tau_{LA}^{(U)}(\omega)$ ($\sim 1/\omega^4$) compared to that for N scattering

($\sim 1/\omega^2$) leads in a natural way to the cross-over behavior. We note that our result $\tau_j^{RTA}(\omega \rightarrow 0) \sim 1/\omega^2$ is consistent with the commonly used forms¹⁻⁵ originally obtained for low-frequency phonons. In recent decades, many room-temperature RTA calculations for bulk and nanostructured materials have used $\tau_j^{(U)}(\omega) \sim 1/\omega^2$, a much weaker frequency dependence than revealed from our *ab initio* results. This highlights the importance of using a first-principles approach to develop accurate intrinsic phonon relaxation times.

It is interesting to compare the *ab initio* approach used here to one based on molecular dynamics (MD) simulations.²⁴ In the MD approach, phonon relaxation times for solid argon were extracted from the autocorrelation of the phonon mode energies and RTA thermal conductivities were compared to those obtained from a Green Kubo method. The obtained relaxation times also exhibited a $1/\omega^2$ frequency dependence for small ω , but for larger ω they follow either $1/\omega^2$ or $1/\omega$ depending on branch and temperature. This is in contrast to our $1/\omega^4$ high-frequency behavior. As stated above, the behavior we find is consistent with the rapid increase in umklapp scattering with frequency. Many of the umklapp scattering processes that contribute to the scattering rates involve optic modes, which are not present in Argon. This might be one reason for the different obtained frequency dependences from the two approaches.

IV. SUMMARY AND CONCLUSIONS

In summary, we have used a first-principles approach to derive forms for the intrinsic phonon relaxation times describing N and U phonon-phonon scattering around and above room temperature. The different frequency dependences obtained for the N and U scattering reflect the behavior that is qualitatively expected for these physically distinct processes. Our approach has allowed us to illustrate the inaccuracy of the commonly used long wavelength approximation for three-phonon scattering and to examine the validity of the RTA, which we find accurately represents κ_L for Si and Ge.

ACKNOWLEDGMENTS

The authors gratefully acknowledge support from the National Science Foundation under Grant No. CBET 0651381.

¹P. G. Klemens, Proc. R. Soc. London **A208**, 108 (1951).

²C. Herring, Phys. Rev. **95**, 954 (1954).

³J. Callaway, Phys. Rev. **113**, 1046 (1959).

⁴M. G. Holland, Phys. Rev. **132**, 2461 (1963).

⁵G. A. Slack and S. Galginitis, Phys. Rev. **133**, A253 (1964).

⁶M. Asen-Palmer, K. Bartkowski, E. Gmelin, M. Cardona, A. P. Zhernov, A. V. Inyushkin, A. Taldenkov, V. I. Ozhogin, K. M. Itoh, and E. E. Haller, Phys. Rev. B **56**, 9431 (1997).

⁷D. T. Morelli, J. P. Heremans, and G. A. Slack, Phys. Rev. B **66**, 195304 (2002).

⁸N. de Koker, Phys. Rev. Lett. **103**, 125902 (2009).

⁹M. V. Simkin and G. D. Mahan, Phys. Rev. Lett. **84**, 927 (2000).

¹⁰N. Mingo and D. A. Broido, Phys. Rev. Lett. **93**, 246106 (2004).

¹¹W. Kim, J. Zide, A. Gossard, D. Klenov, S. Stemmer, A. Shakouri, and A. Majumdar, Phys. Rev. Lett. **96**, 045901 (2006).

¹²R. Peierls, Ann. Phys. **3**, 1055 (1929).

¹³D. A. Broido, M. Malorny, G. Birner, N. Mingo, and D. A. Stewart, Appl. Phys. Lett. **91**, 231922 (2007).

¹⁴A. Ward, D. A. Broido, D. A. Stewart, and G. Deinzer, Phys. Rev. B **80**, 125203 (2009).

¹⁵S. Baroni, S. de Gironcoli, A. Dal Corso, and P. Giannozzi, Rev. Mod. Phys. **73**, 515 (2001).

- ¹⁶G. Deinzer, G. Birner, and D. Strauch, Phys. Rev. B **67**, 144304 (2003).
- ¹⁷M. Omini and A. Sparavigna, Nuovo Cimento D **19**, 1537 (1997).
- ¹⁸D. A. Broido, A. Ward, and N. Mingo, Phys. Rev. B **72**, 014308 (2005).
- ¹⁹G. P. Srivastava, *The Physics of Phonons* (Adam Hilger, London, 1990), Chap. 5 and 6.
- ²⁰J. Callaway, *Quantum Theory of the Solid State* (Academic Press, San Diego, 1991).
- ²¹S. Baroni *et al.*, <http://www.quantum-espresso.org>.
- ²²G. Nilsson and G. Nelin, Phys. Rev. B **6**, 3777 (1972).
- ²³For large \vec{q} , the anisotropy of $\tau_j^{(i)}(\vec{q})$ means the $\tau_j^{(i)}(\omega)$ are multivalued functions. However, this occurs at values of ω where $\tau_j^{(i)}(\omega)$ is small and the contribution to the thermal conductivity is minimal.
- ²⁴A. J. H. McGaughey and M. Kaviany, Phys. Rev. B **69**, 094303 (2004).